# Neural crest-derived neurons invade the ovary but not the testis during mouse gonad development

Jennifer McKey[a], Corey Bunce[a], Iordan S. Batchvarov[a], David M. Ornitz[b], and Blanche Capel[a,1]

[a]Department of Cell Biology, Duke University Medical Center, Durham, NC 27710; and [b]Department of Developmental Biology, Washington University School of Medicine, St. Louis, MO 63110

Edited by Marianne E. Bronner, California Institute of Technology, Pasadena, CA, and approved February 4, 2019 (received for review August 29, 2018)

**Testes and ovaries undergo sex-specific morphogenetic changes and adopt strikingly different morphologies, despite the fact that both arise from a common precursor, the bipotential gonad. Previous studies showed that recruitment of vasculature is critical for testis patterning. However, vasculature is not recruited into the early ovary. Peripheral innervation is involved in patterning development of many organs but has been given little attention in gonad development. In this study, we show that while innervation in the male reproductive complex is restricted to the epididymis and vas deferens and never invades the interior of the testis, neural crest-derived innervation invades the interior of the ovary around E16.5. Individual neural crest cells colonize the ovary, differentiate into neurons and glia, and form a dense neural network within the ovarian medulla. Using a sex-reversing mutant mouse line, we show that innervation is specific to ovary development, is not dependent on the genetic sex of gonadal or neural crest cells, and may be blocked by repressive guidance signals elevated in the male pathway. This study reveals another aspect of sexually dimorphic gonad development, establishes a precise timeline and structure of ovarian innervation, and raises many questions for future research.**

organogenesis | testis | ovary | neural crest | innervation

The development of the testis and ovary is a unique model of organogenesis in which two distinct organs arise from the same gonadal precursor tissue, the bipotential gonad. At the stage of sex determination, mouse embryonic day 11.5 (E11.5), bipotential gonads commit to a sex-specific fate and develop into testes in XY embryos and ovaries in XX embryos. The striking morphological dimorphism evident between testes and ovaries is initiated by intrinsic pathways controlled by the sex determination cascade and, at least in the case of the testis, propagated by differential recruitment of extrinsic components involved in patterning the organ.

An interaction between the male pathway and the vasculature instructs testis patterning. Vasculature migrates from the mesonephros into the testis based on signals initiated by the male pathway (1). Live imaging showed that endothelial cells first migrate to form the coelomic artery at the surface of the testis, then branch and induce proliferation of the surrounding mesenchyme, which separates Sertoli cells into clearly defined testis cords (2, 3). Disruption of endothelial migration led to severe defects in testis morphogenesis and cord formation (2, 4). These results demonstrated the essential role of endothelial cell migration in patterning the testis. However, recruitment of external vasculature did not occur into the ovary during the stages investigated in these studies (1, 3), thus seemed unlikely to be involved in early patterning events of the ovary, such as germ cell cyst formation and breakdown to form primordial follicles (5, 6). The factors regulating ovary patterning remain largely unknown.

Peripheral innervation is another extrinsic component that is involved in organ patterning during development (7, 8), but has been given little attention in gonad development. To the best of our knowledge, there have been no studies on innervation of the mouse testis. While older studies identified neural projections present inside the medulla of the mammalian ovary in fetal and adult life in the mouse and human ovary (9–12), these studies were performed on ovary sections and thus did not provide an integrative view of ovarian innervation in the three-dimensional context of the gonad/mesonephric complex. The majority of the peripheral nervous system is derived from the neural crest progenitor population that colonizes target organs during embryonic development (13). A recent study demonstrated the pathways of sacral neural crest migration into the lower urogenital tract (14); however, the gonads were not studied.

Here we lineage-traced the neural crest and compared the development of innervation in the male and female gonad/mesonephric complex. We show that neural crest cell (NCC) derived neural projections enter the dorsal mesonephros of both male and female embryos at E15.5. The innervation then invades the dorsal face of the ovary at E16.5. From E18.5 onward, a dense neural network forms within the developing ovarian medulla. In contrast, innervation in the testis is restricted to the tunica, the epididymis, and vas deferens and never invades the interior of the testis. Similar to sexual dimorphism in vascular development, dimorphism in gonad innervation is controlled by pathways downstream of the commitment of the gonad to male or female fate and may be critical for morphogenesis or function of the ovary.

## Results

**Innervation Arrives Near the Gonads at E15.5.** At E15.5, innervation of the mouse urogenital system is already well developed. Staining for the neural body marker HuC/D and the pan-neuronal marker TUJ1 showed that the ganglia from the sympathetic chain already extend a number of projections into the adrenal glands and kidneys (Fig. 1 *A* and *B*). In both XX and XY embryos, neural

### Significance

This study investigates the sexually dimorphic development of innervation in mouse gonads. Neural crest-derived neurons invade the dorsal surface of the mouse ovary during embryonic development and give rise to a neural network, whereas in males, innervation is restricted to the surface of the testis. We propose a molecular mechanism regulating sexual dimorphism in this aspect of gonad development. Growing evidence indicates that neural crest cells can instruct patterning of their target organs during development, independently of their role in the adult organ. The structure and developmental timeline of male and female innervation established in this study lay the groundwork for characterization of functional interactions between neural and other cell types during gonad and duct patterning.

Author contributions: J.M. and B.C. designed research; J.M., C.B., and I.S.B. performed research; D.M.O. contributed new reagents/analytic tools; J.M. and C.B. analyzed data; and J.M. and B.C. wrote the paper.

The authors declare no conflict of interest.

This article is a PNAS Direct Submission.

Published under the PNAS license.

[1]To whom correspondence should be addressed. Email: blanche.capel@duke.edu.

This article contains supporting information online at www.pnas.org/lookup/suppl/doi:10.1073/pnas.1814930116/-/DCSupplemental.

Published online February 28, 2019.

projections from the celiac ganglia extend posterior to the kidney, toward the mesonephros (Fig. 1 *A* and *B*). Using printed slides designed for imaging both the dorsal and ventral surfaces (*SI Appendix*, *SI Materials and Methods*and *SI Appendix*, Fig. S1), we acquired images of gonad–mesonephros complexes stained with TUJ1 and the granulosa cell marker FOXL2 in XX samples (Fig. 1 *C* and *D*) or the Sertoli cell marker AMH in XY samples (Fig. 1 *E* and *F*). Results confirmed that at E15.5, TUJ1-positive neural projections had reached the dorsal face of the mesonephros in both XY and XX embryos. In addition, we noted the presence of two groups of five to eight cells positive for both HuC/D and TUJ1 in the anterior and posterior extremities of the XX mesonephros (Fig. 1 *C* and *C′*) and in the posterior extremity of the XY mesonephros (Fig. 1 *E* and *E′*), suggesting that individual neurons were present in the mesonephros at this stage. Some TUJ1 staining was observed in the Sertoli cells of the testes (Fig. 1*F′*), as previously reported (15). However, no innervation-specific signal was detected inside the gonads of either XY or XX samples (Fig. 1 *C*–*F*).

**Innervation Invades the Ovary but Not the Testis.** At E16.5, comparison of TUJ1 immunostaining on the ventral side (Fig. 2 *A* and *B*) and dorsal side (Fig. 2 *C* and *D*) of both XY and XX samples demonstrated that innervation occurs mainly on the dorsal face of the gonad–mesonephros complex. In XY samples, TUJ1+ staining extends into the developing efferent ductules, epididymis, and vas deferens. However, the innervation stayed at a distance from the testis, which was marked by AMH immunostaining (Fig. 2*C*). In XX samples, TUJ1-positive neural projections had expanded in the mesonephros and began to invade the dorsal face of the developing ovary, which was stained with antibodies against FOXL2 (Fig. 2*D*). At E18.5, a network of neural projections continued to develop in the epididymis and vas deferens of XY samples. However, there was still no innervation in the interior domain of the testis (Fig. 2*E*). We detected some TUJ1 projections within the tunica albuginea on the surface of the testis, but optical slices from a plane 28 μm deeper into the tissue confirmed that neural projections were restricted to the surface and did not invade the interior of the organ (Fig. 2*E′*). In contrast, in XX samples, innervation had invaded the dorsal face of the ovary, and TUJ1-positive neural projections formed a neural network detectable deep within the FOXL2-positive domain (Fig. 2 *F* and *F′*). In neonatal mice (postnatal day 0, P0), while the testis still had no internal innervation (Fig. 2*G*), the ovarian neural network had expanded and appeared now to be connected to the innervation of the mesonephros through the developing hilus (Fig. 2*H*). We cleared P0 testes and ovaries and used light sheet microscopy to image the entire cleared gonads immunostained for TUJ1 and the gonad marker GATA4. This confirmed the absence of innervation inside the testis at this stage (Movie S1) and the presence of a neural network within the ovary (Movie S2). Finally, at P5, there was still no detectable neural-specific stain inside the testis (Fig. 2*I*), whereas the ovarian innervation presented a dense neural network within the medulla (Fig. 2 *J* and *J′*). At this stage, the innervation was also detectable in images taken from the ventral face of the ovary, demonstrating that the neural projections had grown from the ovarian medulla out to the cortical region (Fig. 2 *K* and *K′*). In many systems, innervation and vasculature tend to overlap and follow similar paths during development and invasion of target organs. To investigate whether this is the case during gonad development, we studied the expression of endothelial markers ENDOMUCIN and PECAM compared with the expression of the neural reporter *Doublecortin-DsRed* (*Dcx-DsRed*), and TUJ1 (*SI Appendix*, Fig. S2). We found that during XY gonad development, the vasculature was already strongly patterned at E15.5 and did not undergo significant changes between E15.5 and P0 (*SI Appendix*, Fig. S2 *A*–*C*). The expression of the *Dcx-DsRed* reporter throughout this time-course confirmed with a second neural marker that innervation in the XY gonad is restricted to the epididymis and vas deferens and does not invade the interior of the testis (*SI Appendix*, Fig. S2 *A″*, *B″*, and *C″*). In the XX gonad (*SI Appendix*, Fig. S2 *D*–*F*), comparison of ENDOMUCIN staining with expression of the *Dcx-DsRed* reporter revealed that vasculature precedes innervation within the developing ovary (*SI Appendix*, Fig. S2*D*). At E17.5, we found that ENDOMUCIN and DsRed expression overlapped in the posterior end of the XX gonad (*SI Appendix*, Fig. S2*E*), suggesting that vasculature and innervation share a point of entry into the ovary. However, at P0, expression of ENDOMUCIN and DsRed did not completely overlap inside the XX gonad (*SI Appendix*, Fig. S2*F*), suggesting that once in the ovary, vasculature and innervation follow different patterns. Comparison of the pan-endothelial marker PECAM with the pan-neuronal marker TUJ1 led to similar observations (*SI Appendix*, Fig. S2 *G* and *H*).

In some cases, immunostaining of female samples with antibodies against the neural body marker HuC/D revealed the presence of a bouquet of positive cells in the anterior portion of the ovary (Fig. 2 *L*–*O*). This ganglion-like structure was most often observed in samples of E17.5 (Fig. 2 *L* and *M*) to P0 embryos (Fig. 2 *N* and *O*) and included neural projections that extended into the medullary region of the ovary and appeared to connect to the mesonephric innervation. In Fig. 2 *N* and *O*, HuC/D signal is detected in the oocyte cytoplasm. In fact, the HuC/D

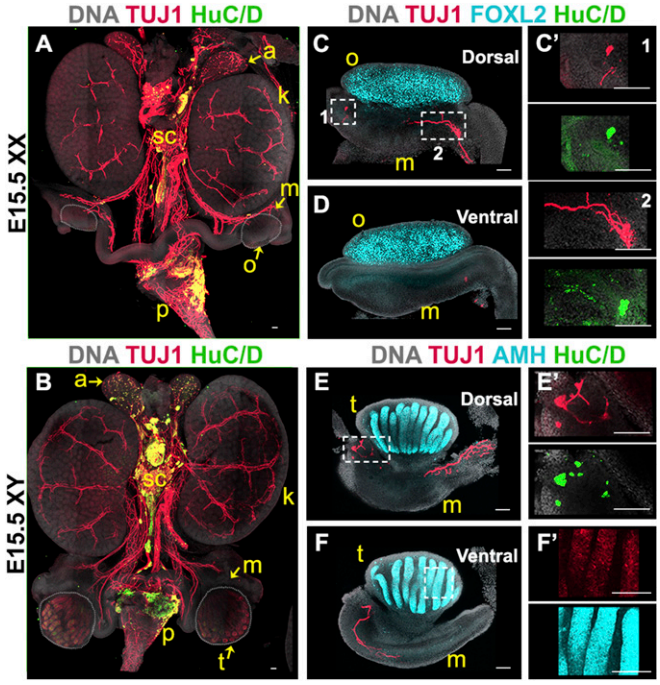


**Fig. 1.** Innervation reaches the gonad/mesonephros complex at E15.5. Whole-mount fluorescent immunostaining. (*A* and *B*) Urogenital complexes from E15.5 XX (*A*) or XY (*B*) embryos. The bladder was removed at dissection for better visualization. To best visualize the gonads, the XX sample (*A*) was imaged from the dorsal side, and the XY sample (*B*) was imaged from the ventral side. (*C*–*F*) E15.5 gonads from XX (*C* and *D*) or XY (*E* and *F*) embryos imaged from the dorsal (*C* and *E*) or ventral (*D* and *F*) side. (*C′*) Magnified views (1 and 2) of the areas outlined in *C*. *E′* and *F′* are magnified views of the areas outlined in *E* and *F*. Samples were stained for the pan-neuronal marker TUJ1 (red, *A*–*F*) and neural body marker HuC/D (green, *A*–*F*). XX samples were stained for the granulosa cell marker FOXL2 to label the ovary (cyan, *C* and *D*), and XY samples were stained for the Sertoli cell marker AMH to label the testis (cyan, *E* and *F*). All samples were counterstained with Hoechst nuclear dye (grayscale). a, adrenal gland; k, kidney; m, mesonephros; o, ovary; p, pelvis; sc, sympathetic chain; t, testis. (Scale bars, 100 μm.)

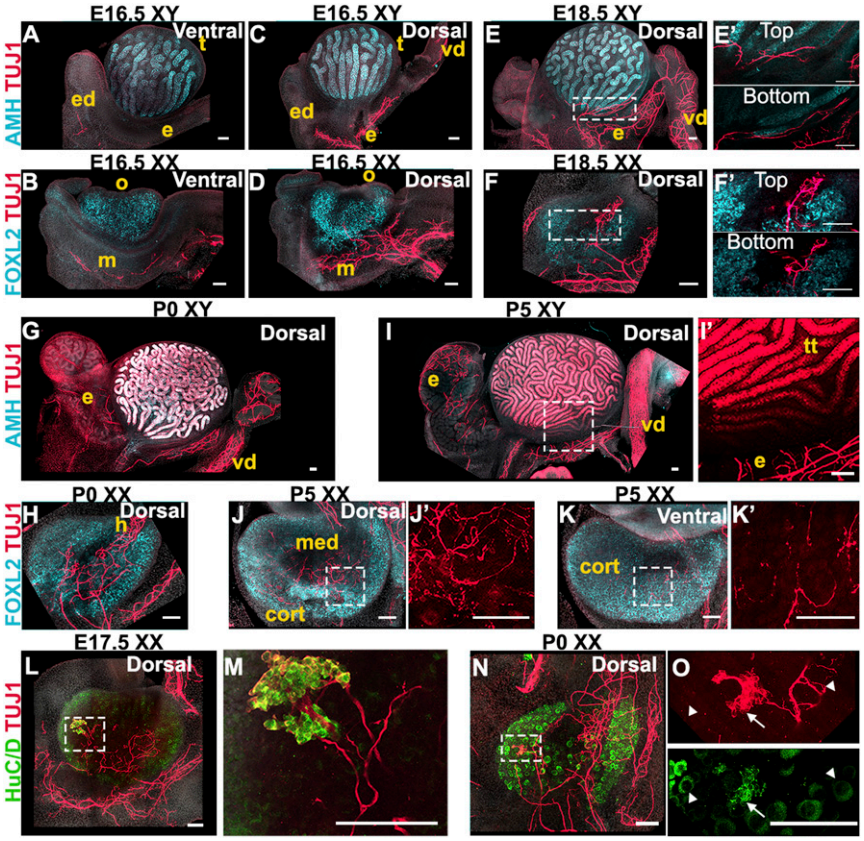


**Fig. 2.** Innervation invades the interior of the ovary but not the testis. (*A*–*D*) E16.5 XY (*A* and *C*) or XX (*B* and *D*) gonads imaged from the ventral (*A* and *B*) or dorsal (*C* and *D*) side. (*E* and *F*) E18.5 XY (*E*) or XX (*F*) gonads imaged from the dorsal side. *E*′ and *F*′ are magnified views of the areas outlined in *E* and *F* that represent the *Top* and *Bottom* (28 μm deeper) optical sections from the Z-stacks used to generate maximum-intensity projections shown in *E* and *F*. (*G* and *H*) P0 XY (*G*) or XX (*H*) gonads imaged from the dorsal side. (*I*–*K*) P5 XY (*I*) or XX (*J* and *K*) gonads imaged from the dorsal (*I* and *J*) or the ventral side (*K*). *I*′, *J*′, and *K*′ are magnified views of TUJ1 staining from the areas outlined in *I*, *J*, and *K*. Note that TUJ1 also stains Sertoli cells at some stages (*I* and *I*′). (*L*–*O*) E17.5 (*L* and *M*) and P0 (*N* and *O*) XX gonads stained for the pan-neuronal marker TUJ1 (red, *A*–*O*) and neural body marker HuC/D (green, *L*–*O*). *M* and *O* are higher-magnification images of the areas outlined in *L* and *N*. Note that HuC/D also stains oocytes (*L*–*O* and *SI Appendix*, Fig. S3). HuC/D staining in the oocyte is distinct from the stain observed in neural bodies: white arrowheads in *O* point to TUJ1-/HuC/D+ oocytes, and white arrows in *O* point to TUJ1+/HuC/D+ neural cell bodies. XY samples were stained for the Sertoli cell marker AMH (cyan, *A*, *C*, *E*, *G*, and *I*), and XX samples were stained for the granulosa cell marker FOXL2 (cyan, *B*, *D*, *F*, *H*, *J*, and *K*). All samples were counterstained with Hoechst nuclear dye (grayscale). cort, cortex; e, epididymis; ed, efferent ductules; h, hilus; m, mesonephros; med, medulla; o, ovary; t, testis; tt, testis tubules; vd, vas deferens. (Scale bars, 100 μm.)

antibody stained female germ cells throughout the time-course observed in this study (*SI Appendix*, Fig. S3).

**Gonad Innervation Is Neural Crest-Derived.** To determine whether gonad innervation is neural crest-derived, we performed lineage tracing of neural crest cells using *Wnt1Cre; Rosa-tdTomato* mice. As expected, we found that all of the TUJ1-positive neural projections overlapped with tdTomato expression in the urogenital system, including the gonad /mesonephros complexes of both sexes at E15.5 (Fig. 3 *A* and *B*). We next stained *Wnt1cre; Rosa-tdTomato* gonad samples at P0 for the neural marker doublecortin (DCX) and found that all DCX-positive neural projections were also positive for tdTomato in the XY epididymis and vas deferens (Fig. 3*C*). A network of NCC-derived innervation was detected in the cauda of the vas deferens (Fig. 3*C*′). In the ovary, the DCX signal overlapped completely with tdTomato expression, demonstrating that the entire ovarian neural network is neural crest-derived (Fig. 3 *D* and *D*′).

**Neural Crest-Derived Progenitors Colonize the Ovary and Differentiate into Neurons and Glia.** We found that individual tdTomato-positive cells invade the posterior region of the ovary at E16.5 (Fig. 4 *A* and A′). These cells did not appear to have any connection to the axonal projections extending from the mesonephros, suggesting that not only does the mesonephric innervation project into the ovary, but also that individual NCCs migrate directly into the ovary. Colocalization of tdTomato and HuC/D in the anterior region of the ovary at E17.5 (Fig. 4 *B* and *B*′) and P0 (Fig. 4 *C* and *C*′) confirmed that the ganglion-like structure previously detected (Fig. 2 *L*–*O*) is neural crest-derived.

Not all tdTomato-positive cells inside the ovary were stained with DCX (Fig. 3*D*). This could mean that not all NCCs have differentiated by P0 or that another population of NCC-derived cells is present in the ovary. During the establishment of the peripheral nervous system, NCCs contribute both the neurons and the glial cells that support peripheral neural activity (13). To determine whether the tdTomato+/DCX- cells observed in the ovary are differentiated glial cells, we compared the expression of S100b, a glial cell marker, to nerve fibers in *Wnt1Cre; Rosa-tdTomato* gonads. We found that at E17.5 and P5, tyrosine hydroxylase-positive nerve fibers extending into the developing ovary are surrounded by cells double-positive for tdTomato and S100b (Fig. 4 *D* and *E*), indicating that NCC-derived glial cells are present within the ovary from the beginning of the formation of the ovarian neural network.

**NCC Migration Is Dependent on Gonadal Fate Rather than Genetic Sex.** Our results show that NCCs invade the ovary but not the testis. To determine whether this results from the genetic sex of

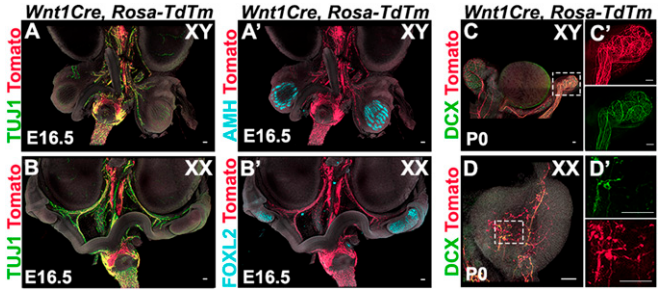


**Fig. 3.** Gonad innervation is neural crest-derived. (*A* and *B*) Lineage-trace of neural crest-derived neurons in whole urogenital complexes from XY (*A*) and XX (*B*) *Wnt1Cre; Rosa-tdTomato* embryos at E15.5. (*C* and *D*) Lineage-trace of neural crest-derived progenitors in gonads from XY (*C*) and XX (*D*) *Wnt1Cre; Rosa-tdTomato* neonates (P0). *C′* and *D′* are magnified views in single channels of the areas outlined in *C* and *D*. Samples were stained for red fluorescent protein (RFP) to detect tdTm expression (red, *A* and *D*), the pan-neuronal marker TUJ1 (green, *A* and *B*), and the pan-neuronal marker DCX (green, *C* and *D*). XY samples were stained for the Sertoli cell marker AMH to label the testis (cyan, *A′*), and XX samples were stained for the granulosa cell marker FOXL2 to label the ovary (cyan, *B′*). All samples were counterstained with Hoechst nuclear dye (grayscale). (Scale bars, 100 μm.)

the embryo (either the gonad or the neural crest) or is the result of downstream pathways activated during commitment to ovarian fate, we exploited a sex-reversing mutant. A previous study showed that $Fgf9^{-/-}$ embryos present with male-to-female sex reversal. In these mice, sex reversal occurs after the stage of sex determination, between E12.5 and E14.5, when testis specification and organogenesis have already begun (16). For this experiment, we used the $Fgf9^{lacZ}$ mouse line generated by Huh and collaborators (17), a new gene replacement line that mirrors sex reversal in a timeline similar to that observed in the original $Fgf9^{-/-}$ line (*SI Appendix*, Fig. S4). To investigate gonad innervation in these mutants, we studied embryos at E17.5, a stage where innervation is present in the wild-type ovary and when $Fgf9^{lacZ/lacZ}$ embryos are viable. FOXL2 staining in XX samples from $Fgf9^{lacZ/+}$ (Fig. 5*A*) and $Fgf9^{lacZ/lacZ}$ (Fig. 5*B*) was similar, demonstrating that loss of *Fgf9* does not affect female gonad development. TUJ1 staining of the ovarian neural network in these samples was also comparable (Fig. 5 *A* and *B*). In $Fgf9^{lacz/+}$ XY samples, the testis developed normally, presenting with AMH-positive clearly defined testis cords and no TUJ1-positive innervation within the gonad (Fig. 5*C*). However, by E17.5, XY $Fgf9^{lacZ/lacZ}$ gonads had developed into ovaries, as demonstrated by the expression of FOXL2 (Fig. 5*D*). In addition, TUJ1 staining revealed a neural network inside the gonad (Fig. 5*D*). Thus, male-to-female sex reversal in *Fgf9* mutants leads to innervation of an XY ovary, indicating that NCCs invade the XY gonad soon after the ovarian pathway is activated, regardless of the initial steps of testis organogenesis that occur in $Fgf9^{lacZ/lacZ}$ XY gonads.

In other systems, migrating NCCs are attracted by guidance cues expressed by their target organs and repelled by avoidance cues to ensure they do not invade ectopic locations (18–20). We hypothesized that the ovary may express cues to attract neural crest-derived progenitors, and/or the testis may express repulsive cues to avoid invasion. We first interrogated a time-course transcriptome dataset (21) for common NCC guidance cues and found that many of them became differentially expressed in male and female gonads at E12.5, 24 h after sex determination occurs (*SI Appendix*, Fig. S5). RT-qPCR analysis of XY and XX gonads at E14.5 and E16.5 showed that expression remained dimorphic at the stages most relevant for neural invasion of the gonads (Fig. 5*E*). While attractive cues were not enriched in XX gonads, we found that expression of the repulsive neural crest guidance cues *Sema3f*, *Sema6c*, and *Slit3* was significantly higher in E16.5 XY versus XX gonads (Fig. 5*E*). We next compared the expression of these candidate repulsive cues in *Fgf9* sex-reversing mutants at E16.5. We found that expression of *Sema3f*, *Sema6c*, and *Slit3* was down-regulated near XX levels in sex-reversed $Fgf9^{lacZ/lacZ}$ XY gonads compared with heterozygous XY littermates (Fig. 5*F*).

## Discussion

Soon after gonadal sex determination (E11.5-E12.5), testis and ovary morphology begin to diverge. Previous experiments showed that recruitment of extrinsic vasculature is specific to the testis, where it is required for morphological patterning of the organ (1–3). Here we show in a parallel set of experiments that recruitment of a neuronal network is specific to the ovary.

Individual NCCs colonize the ovary around E16.5 and differentiate into neurons and glia that give rise to the entire ovarian neural network (Fig. 6). In contrast, NCCs do not invade the testis. This could have been explained by an inability of XY neural crest cells to respond to gonadal cues. To test this possibility, we first performed XX/XY gonad/mesonephros tissue recombinations in organ culture in which a *Wnt1Cre; Rosa-Tm*–labeled female mesonephros was recombined at E16.5 with a wild-type testis or a male *Wnt1Cre; Rosa-Tm*–labeled mesonephros was recombined with an ovary. However, these experiments were inconclusive, as the development and patterning of the ovarian neural network was lost in culture, most likely as a result of severing the link from the sympathetic chain during dissection.

We next turned to a genetic model of male-to-female sex reversal to address this question. $Fgf9^{lacZ/lacZ}$ XY gonads initiate testis organogenesis but undergo sex reversal around E12.5 and initiate ovary development (16). We found that $Fgf9^{lacZ/lacZ}$ XY

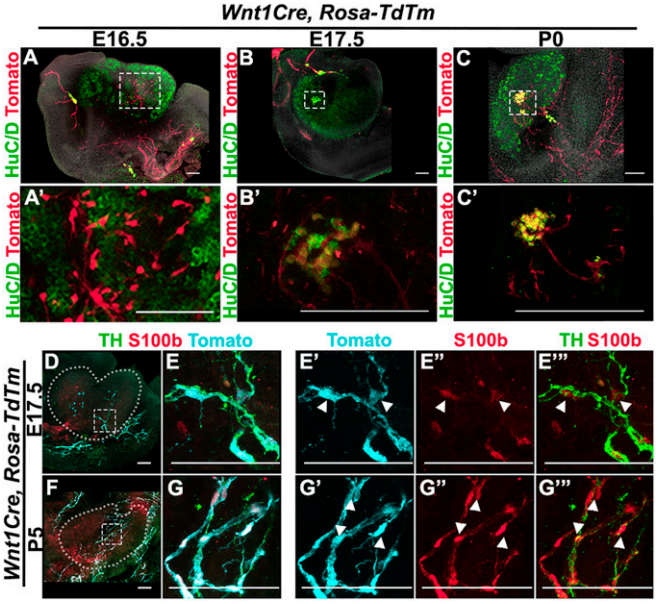


**Fig. 4.** Neural crest-derived progenitors colonize the ovary and differentiate into neurons and glia. (*A*–*C*) Lineage-trace of neural crest-derived progenitors in gonads from XX *Wnt1Cre; Rosa-tdTomato* embryos at E16.5 (*A*), E17.5 (*B*), and P0 (*C*). *A′*, *B′*, and *C′* are magnified views of the areas outlined in *A*, *B*, and *C*. Samples were stained for red fluorescent protein (RFP) to detect tdTm expression (red), the neural body marker HuC/D (green), and counterstained with Hoechst nuclear dye (grayscale). (*D*–*G*) Lineage-trace of neural crest-derived neurons and glia in gonads from XX *Wnt1Cre; Rosa-tdTomato* embryos at E17.5 (*D* and *E*) and P5 (*F* and *G*). (*E* and *G*) Higher-magnification images of the areas outlined in *D* and *F*. Subsequent panels in each row show selected channels from the merged channels shown in *E* and *G*. Samples were stained for RFP to detect tdTm expression (cyan), the neural marker Tyrosine Hydroxylase (TH) (green), and the glial cell marker S100b (red). White arrowheads in *E′* and *G′* series point to tdTm+/S100b+/TH- cells in the ovary. (Scale bars, 100 μm.)

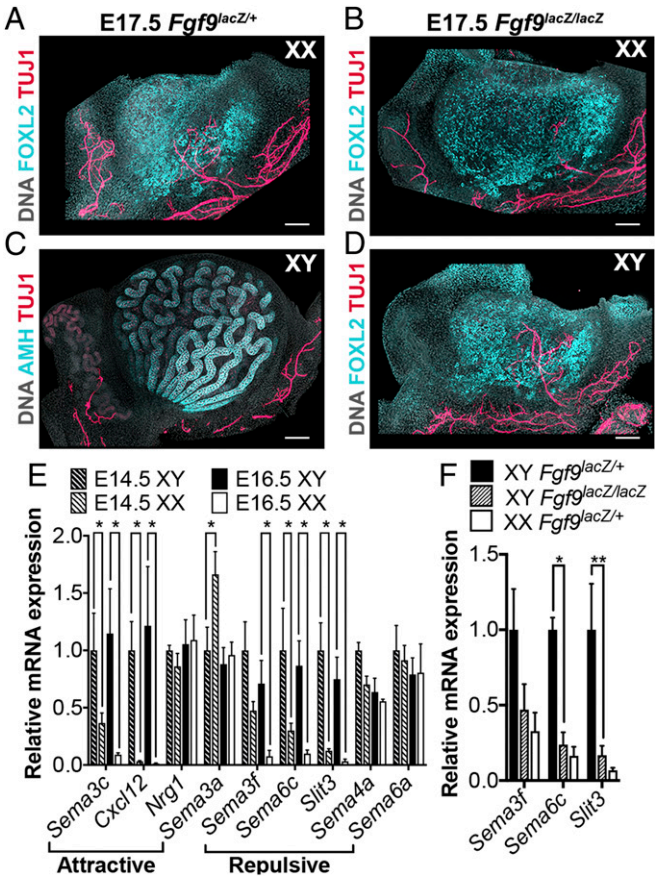


**Fig. 5.** Neural crest migration is dependent on gonadal fate rather than genetic sex. (*A* and *B*) XX gonads from E17.5 $Fgf9^{lacZ/+}$ (*A*) and $Fgf9^{lacZ/lacZ}$ (*B*) embryos. (*C* and *D*) XY gonads from E17.5 $Fgf9^{lacZ/+}$ (*C*) or $Fgf9^{lacZ/lacZ}$ (*D*) embryos. All samples were stained for the pan-neuronal marker TUJ1 (red), and counterstained with Hoechst nuclear dye (grayscale). XX samples and $Fgf9^{lacZ/lacZ}$ XY samples were stained for the granulosa cell marker FOXL2 to label the ovary (cyan, *A*, *B*, and *D*). $Fgf9^{lacZ/+}$ XY samples were stained with the Sertoli cell marker AMH to label the testis (cyan, *C*). (Scale bars, 100 μm.) (*E*) RT-qPCR analysis of relative mRNA expression of common neural crest attractive (*Semaphorin 3c*, *Cxcl12*, *Neuregulin 1*) or repulsive (*Semaphorins 3a, 3f, 4a, 6a, 6c*, and *Slit3*) cues in gonads from E14.5 (dashed bars) and E16.5 (solid bars) XY (black bars) or XX (white bars) embryos. Data were normalized to *Gapdh* expression. Values presented are the mean ± SEM of $n = 4$ pairs of gonads converted to fold changes compared with E14.5 XY samples for each gene. $^*P < 0.05$ by two-tailed standard *t* test. (*F*) RT-qPCR analysis of relative mRNA expression of *Semaphorins 3a, 6c*, and *Slit3* in gonads from E16.5 XY $Fgf9^{lacZ/+}$ (black bars), XY $Fgf9^{lacZ/lacZ}$ (dashed bars), or XX $Fgf9^{lacZ/+}$ (white bars) embryos. Data were normalized to *Gapdh* expression. Values presented are the mean ± SEM of $n = 3$ pairs of gonads converted to fold changes compared with XY $Fgf9^{lacZ/+}$ samples for each gene. $^*P < 0.05$; $^{**}P < 0.01$ by two-tailed standard *t* test.

ovaries are innervated similar to wild-type ovaries, demonstrating that XY NCCs are capable of colonizing gonadal tissue, and XY ovarian tissue is permissive for NCC invasion. These results indicate that the sexually dimorphic behavior of the neural crest depends either on attractive cues expressed in the ovary pathway or repulsive cues activated in the testis pathway. The attractive cues present in the E11.5-E13.5 dataset (21) were not significantly enriched in XX gonads at E14.5 or E16.5 (the relevant stages for neural crest invasion). However, several neural crest avoidance cues were highly enriched in XY gonads at these stages. Among these, *Sema3f* and *Slit* molecules have both been described as repulsive cues for trunk NCCs (18, 22), which is likely the population that innervates the urogenital complex. These findings have led to the hypothesis that the sexually dimorphic behavior of NCC-derived progenitors is due to repulsive cues activated in the male pathway. In support of this hypothesis, we show that *Sema3f*, *Sema6c*, and *Slit3* are all down-regulated in sex-reversed XY ovaries. In fact, expression levels in homozygous XY gonads was similar to that of heterozygous XX gonads, consistent with a role for these repulsive cues in establishing sexually dimorphic gonad innervation. Functional investigation of these genes will be performed in future experiments.

Why is a neuronal network established in the interior of the ovary, but restricted to the tunica albuginea of the testis? Why is a neuronal network not required within the testis? Does another cell type in the testis, such as the neuroendocrine Leydig cells (23, 24) or tissue macrophages (15, 25), take over the role of systemic communication? While we have yet to address these questions regarding the testis, this study narrows the path toward a functional understanding of ovarian innervation.

Recruitment of neural crest-derived neurons and glia into the ovary coincides with critical patterning events during ovary development, including rotation of the cortex to the ventral surface of the ovary, establishment of the hilus, germ cell cyst breakdown (6), primordial follicle formation (26), and activation of the first wave of growing follicles soon after birth (27). A growing number of studies have shown that neural crest-derived cells can instruct the patterning and differentiation of their target tissues during embryonic development, independently from their role in the adult organ (7, 8). Interestingly, the first wave of follicle activation that occurs around birth begins on the dorsal side of the ovary (27), where the ovarian neural network initially develops. It will be important to investigate whether this is only a correlation or whether innervation participates in regulating this first wave of follicle activation. Mesenchyme-derived theca cells, the steroidogenic cells of the ovary, also migrate into the ovary between E17.5 and P5 in a pattern very similar to the development of ovarian innervation (28). In the ovary, neural projections are located in close proximity to the theca layer of the growing follicles (11), where they may be involved in stimulating theca or smooth muscle cells during follicle growth and ovulation (29).

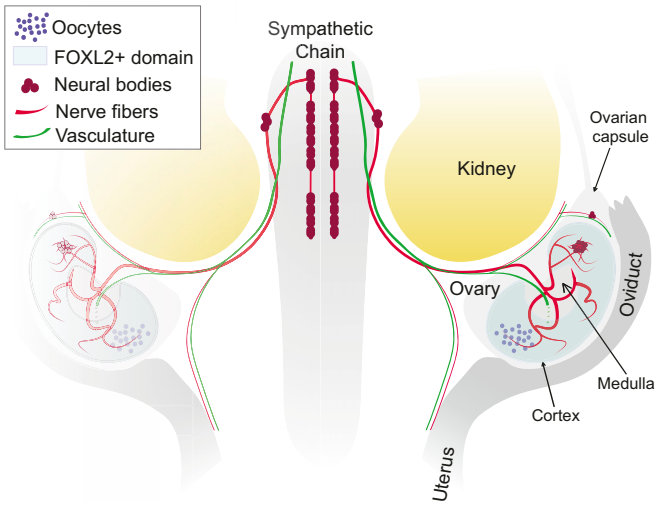


**Fig. 6.** Innervation of the fetal mouse ovary. Neural crest-derived nerve fibers extend from the sympathetic chain posterior to the kidney and into the ovary. Neural crest-derived neural bodies are present in the anterior region of the ovarian capsule and also within the anterior region of the ovary. The ovarian neural network is dense in the ovarian medulla, a region without ovarian follicles, and extends projections across the FOXL2+ toward the ovarian cortex. While vasculature and innervation follow similar tracks to the ovary, they exhibit different patterns once inside the ovary.

Future studies should address whether migrating theca cells express known neural guidance cues and whether these two migratory populations interact and/or rely on each other during ovary development. Although there is evidence that lack of proper innervation in the ovary leads to disruptions of ovarian physiology (30, 31), we are still far from understanding how functional interactions are established between ovarian and neuronal cells and how they may be important for regulating ovarian function.

While it had been shown previously that neurons are present in the developing and adult ovary, limitations in lineage tracing and imaging technologies had made it impossible to resolve the ovarian neural network in the context of the whole ovary. Here we describe several key features of the development of innervation in the gonads. These include the precise timeline of innervation development, the differences in the dorsal and ventral surface of the ovary, the neural crest origin of gonad innervation and the ganglion-like structure in the ovary, and whole-mount images that illustrate the innervation in the context of the urogenital complex and the sympathetic chain. Importantly, we provide evidence of the sexual dimorphism in gonad innervation. While innervation in the male reproductive complex is restricted to the epididymis and vas deferens and never invades the interior of the testis, neural crest-derived innervation invades the interior of the ovary around E16.5. We suggest that sexual dimorphism of gonadal innervation is attributable to repressive cues that block invasion of the neural crest into the testis, a hypothesis that will be tested in future experiments.

## Materials and Methods

**Mice.** Unless otherwise stated, experiments were performed on wild-type C57BL/6 embryos. All transgenic lines were maintained on the C57BL/6 background. The *Cg-E2f1*$^{Tg(Wnt1\text{-}cre)2Sor/J}$ (*Wnt1Cre*) and *Gt(ROSA)26Sor*$^{tm14(CAG\text{-}tdTomato)Hze}$*/J (Rosa-tdTomato)* lines were purchased from Jackson Laboratory (Jax stock #022137 and 007914). The *Tg(Dcx-DsRed)14Qlu/J* (*Dcx-DsRed*) reporter line was kindly provided by Debra Silver (Duke University). The *Fgf9*$^{lacZ}$ line was generated using targeted ES cells purchased from the KOMP repository (project #24486), followed by Cre-mediated excision of the Neo selection cassette (17). To obtain embryos at specific stages of development, males were set up in timed mating with several females. Each female was checked daily for the presence of a vaginal plug. Date of plug was considered embryonic day 0.5. All mice were housed in accordance with National Institutes of Health guidelines, and experiments were conducted with the approval of the Duke University Medical Center Institutional Animal Care and Use Committee.

**Immunostaining.** Embryonic gonads were dissected in PBS, fixed in 4% PFA/PBS for 30 min at room temperature (RT) or overnight at 4 °C, and gradually dehydrated into 100% methanol for storage at −20 °C. After gradual rehydration into PBS, tissues were permeabilized in PBS 0.1% TritonX-100 for 1 h at RT and transferred into blocking solution (PBS 1% TritonX-100, 3% BSA, 10% horse serum—for gonads at stages before E14.5, blocking solution was made with 0.1% TritonX-100) for 2 h. Samples were then incubated with primary antibodies diluted in blocking solution overnight at 4 °C. Following three 1-h washes in PBS 0.1% TritonX-100, tissues were incubated with secondary antibodies diluted in blocking solution overnight at 4 °C. Tissues were then washed once in PBS 0.1% TritonX-100 for 30 min and twice in PBS for 30 min and mounted for imaging in polyvinyl alcohol-mounting solution and stored at 4 °C until imaged. To image the dorsal and ventral sides of the same sample, we designed 3D-printed reversible slides that can be flipped and imaged from both sides (*SI Appendix*, Fig. S1). The 3D model is available for download on the NIH 3D Print Exchange website at https://3dprint.nih.gov/discover/3DPX-009765. For information on the primary and secondary antibodies used in this study, see *SI Appendix*, Tables S1 and S2. For additional methods, see *SI Appendix, SI Materials and Methods*.

**ACKNOWLEDGMENTS.** We thank Debra Silver from Duke University for providing us with the *Dcx-DsRed* mouse line. We also thank Vanda Lennon from Mayo Clinic for the HuC/D antibody. We are grateful to all members of the B.C. laboratory for helpful discussions and suggestions on the project. We would like to acknowledge Danielle Maatouk, who was the first to observe the sexual dimorphism in gonad innervation. This work was supported by a grant from the National Institutes of Health (Grant 1R01HD090050-0) (to B.C.). J.M. was supported by postdoctoral fellowships from the Fondation ARC pour la Recherche contre le Cancer (Award #SAE20151203560) and from the American Cancer Society (Award #130426-PF-17-209-01-TBG). C.B. was supported by a grant from the National Institutes of Health (Grant R37HD039963). Light sheet microscopy was supported by a grant from the National Institutes of Health (Grant 1S10OD020010-01A1) to the Duke Light Microscopy Core Facility and by a voucher from the Duke University School of Medicine.

1. Brennan J, Karl J, Capel B (2002) Divergent vascular mechanisms downstream of Sry establish the arterial system in the XY gonad. *Dev Biol* 244:418–428.
2. Cool J, DeFalco TJ, Capel B (2011) Vascular-mesenchymal cross-talk through Vegf and Pdgf drives organ patterning. *Proc Natl Acad Sci USA* 108:167–172.
3. Coveney D, Cool J, Oliver T, Capel B (2008) Four-dimensional analysis of vascularization during primary development of an organ, the gonad. *Proc Natl Acad Sci USA* 105:7212–7217.
4. Combes AN, et al. (2009) Endothelial cell migration directs testis cord formation. *Dev Biol* 326:112–120.
5. Lei L, Spradling AC (2016) Mouse oocytes differentiate through organelle enrichment from sister cyst germ cells. *Science* 352:95–99.
6. Pepling ME, Spradling AC (2001) Mouse ovarian germ cell cysts undergo programmed breakdown to form primordial follicles. *Dev Biol* 234:339–351.
7. Faure S, McKey J, Sagnol S, de Santa Barbara P (2015) Enteric neural crest cells regulate vertebrate stomach patterning and differentiation. *Development* 142:331–342.
8. Rios AC, Serralbo O, Salgado D, Marcelle C (2011) Neural crest regulates myogenesis through the transient activation of NOTCH. *Nature* 473:532–535.
9. Anesetti G, Lombide P, D'Albora H, Ojeda SR (2001) Intrinsic neurons in the human ovary. *Cell Tissue Res* 306:231–237.
10. D'Albora H, Anesetti G, Lombide P, Dees WL, Ojeda SR (2002) Intrinsic neurons in the mammalian ovary. *Microsc Res Tech* 59:484–489.
11. Dees WL, et al. (2006) Origin and ontogeny of mammalian ovarian neurons. *Endocrinology* 147:3789–3796.
12. Malamed S, Gibney JA, Ojeda SR (1992) Ovarian innervation develops before initiation of folliculogenesis in the rat. *Cell Tissue Res* 270:87–93.
13. Le Douarin NM, Smith J (1988) Development of the peripheral nervous system from the neural crest. *Annu Rev Cell Biol* 4:375–404.
14. Wiese CB, Deal KK, Ireland SJ, Cantrell VA, Southard-Smith EM (2017) Migration pathways of sacral neural crest during development of lower urogenital tract innervation. *Dev Biol* 429:356–369.
15. DeFalco T, et al. (2015) Macrophages contribute to the spermatogonial niche in the adult testis. *Cell Rep* 12:1107–1119.
16. Colvin JS, Green RP, Schmahl J, Capel B, Ornitz DM (2001) Male-to-female sex reversal in mice lacking fibroblast growth factor 9. *Cell* 104:875–889.
17. Huh S-H, Warchol ME, Ornitz DM (2015) Cochlear progenitor number is controlled through mesenchymal FGF receptor signaling. *eLife* 4:e05921.
18. Gammill LS, Gonzalez C, Gu C, Bronner-Fraser M (2006) Guidance of trunk neural crest migration requires neuropilin 2/semaphorin 3F signaling. *Development* 133:99–106.
19. Vega-Lopez GA, Cerrizuela S, Aybar MJ (2017) Trunk neural crest cells: Formation, migration and beyond. *Int J Dev Biol* 61:5–15.
20. Young HM, Anderson RB, Anderson CR (2004) Guidance cues involved in the development of the peripheral autonomic nervous system. *Auton Neurosci* 112:1–14.
21. Jameson SA, et al. (2012) Temporal transcriptional profiling of somatic and germ cells reveals biased lineage priming of sexual fate in the fetal mouse gonad. *PLoS Genet* 8:e1002575.
22. Zuhdi N, et al. (2015) Slit molecules prevent entrance of trunk neural crest cells in developing gut. *Int J Dev Neurosci* 41:8–16.
23. Davidoff MS, Schulze W, Middendorff R, Holstein AF (1993) The Leydig cell of the human testis–A new member of the diffuse neuroendocrine system. *Cell Tissue Res* 271:429–439.
24. Sklebar D, Semanjski K, Kos M, Sklebar I, Jezek D (2008) Foetal Leydig cells and the neuroendocrine system. *Coll Antropol* 32:149–153.
25. Hume DA, Halpin D, Charlton H, Gordon S (1984) The mononuclear phagocyte system of the mouse defined by immunohistochemical localization of antigen F4/80: Macrophages of endocrine organs. *Proc Natl Acad Sci USA* 81:4174–4177.
26. Mork L, et al. (2012) Temporal differences in granulosa cell specification in the ovary reflect distinct follicle fates in mice. *Biol Reprod* 86:37.
27. Cordeiro MH, et al. (2015) Geography of follicle formation in the embryonic mouse ovary impacts activation pattern during the first wave of folliculogenesis. *Biol Reprod* 93:88.
28. Liu C, Peng J, Matzuk MM, Yao HH-C (2015) Lineage specification of ovarian theca cells requires multicellular interactions via oocyte and granulosa cells. *Nat Commun* 6:6934.
29. Robker RL, Hennebold JD, Russell DL (2018) Coordination of ovulation and oocyte maturation: A good egg at the right time. *Endocrinology* 159:3209–3218.
30. Luna F, et al. (2003) The effects of superior ovarian nerve sectioning on ovulation in the Guinea pig. *Reprod Biol Endocrinol* 1:61.
31. Morales-Ledesma L, Trujillo A, Apolonio J (2015) In the pubertal rat, the regulation of ovarian function involves the synergic participation of the sensory and sympathetic innervations that arrive at the gonad. *Reprod Biol Endocrinol* 13:61.